This is a preprint, the final version is subject to change, of the American Mineralogist (MSA)
Cite as Authors (Year) Title. American Mineralogist, in press.
(DOI will not work until issue is live.) DOI: http://dx.doi.org/10.2138/am-2016-5560

Revision 1

Crystal structure of a new compound, $CuZnCl(OH)_3$, isostructural with botallackite

Hexing Yang[1,*], Isabel F. Barton[2], Marcelo B. Andrade[1], and Robert T. Downs[1]

[1] Department of Geosciences, University of Arizona, 1040 E. 4th Street, Tucson, Arizona 85721, USA

[2] Lowell Institute for Mineral Resources, University of Arizona, Tucson, AZ 85721, USA

* Corresponding author: hyang@u.arizona.edu

Abstract

A new compound, ideally $CuZnCl(OH)_3$, was found on a metallic mining artifact of copper composition at the Rowley mine, Maricopa County, Arizona, USA, and studied with electron microprobe analysis, single-crystal X-ray diffraction, and Raman spectroscopy. It is isostructural with botallackite [$Cu_2Cl(OH)_3$] with space group $P2_1/m$ and unit-cell parameters a = 5.6883(5), b = 6.3908(6), c= 5.5248(5) Å, β = 90.832(2)°, V = 200.82(3) Å^3. The crystal structure of $CuZnCl(OH)_3$, refined to R_1 = 0.018, is characterized by brucite-type octahedral sheets made of two distinct and considerably distorted octahedra, M1 and M2, which are coordinated by (5OH + 1Cl) and (4OH + 2Cl), respectively. The octahedral sheets are parallel to (100) and connected by O—H···Cl hydrogen bonding. The major structural difference between $CuZnCl(OH)_3$ and botallackite is the complete replacement of Cu^{2+} in the highly angle-distorted M1 site by non-Jahn-Teller distorting Zn^{2+}. The $CuZnCl(OH)_3$ compound represents the highest Zn content ever documented for the atacamite group of minerals, in conflict with all previous reports that botallackite (like atacamite) is the most resistant, of all copper hydroxylchloride $Cu_2Cl(OH)_3$ polymorphs, to the substitution of Zn^{2+} for Cu^{2+}, even in the presence of large excess of Zn^{2+}. Its discovery, along with the recently-described new mineral iyoite, $CuMnCl(OH)_3$, implies that more botallackite-type compounds or minerals with the chemical formula $CuMCl(OH)_3$ (M = Ni^{2+}, Co^{2+}, Fe^{2+}, Mn^{2+}, Cd^{2+}, and Mg^{2+}) may be synthesized or found in nature.

Key words: $CuZnCl(OH)_3$**,** Copper-zinc hydroxychloride, botallackite, atacamite group, crystal structure, Raman spectroscopy

INTRODUCTION

Pure copper hydroxychloride, $Cu_2Cl(OH)_3$, has three reported natural polymorphs: orthorhombic *Pnma* atacamite (Parise and Hyde 1986), monoclinic $P2_1/n$ clinoatacamite (Jambor et al. 1996), and monoclinic $P2_1/m$ botallackite (Hawthorne 1985). In addition, rhombohedral *R*-3 paratacamite, $Cu_3(Cu,Zn)Cl_2(OH)_6$ (Fleet 1975), is known to be stabilized by the partial substitution of Zn^{2+} or Ni^{2+} for Cu^{2+} in one of the four distorted octahedral sites in the structure (Jambor et al. 1996; Grice et al. 1996). The Zn endmember of such a solid solution, $Cu_3ZnCl_2(OH)_6$, crystallizes in either the rhombohedral *R*-3*m* herbertsmithite structure (Braithwaite et al. 2004) or the trigonal *P*-3*m*1 kapellasite structure (Krause et al. 2006).

The $Cu_2Cl(OH)_3$ polymorphs occur commonly as corrosion products of copper and copper-bearing alloys, as well as pigments in wall paintings, manuscript illumination, and other paintings (Scott 2000; Alejandre and Marquez 2006 and references therein). In particular, their formation from the corrosion of bronze and other copper-bearing alloys are the primary cause for the so-called "bronze disease" (see Scott 2000 for a thorough review). Recently, the first copper-containing mineral atacamite was reported in the jaws of the carnivorous marine worm *Glycera* (Lichtenegger et al. 2002), suggesting a possible involvement of biological activities in the formation of $Cu_2Cl(OH)_3$ minerals. Furthermore, the discoveries of various magnetic properties in $Cu_2Cl(OH)_3$ polymorphs have renewed great interest in understanding the correlations between their crystal structures and physical properties (e.g., Takeda et al. 1999; Zheng et al. 2004, 2005, 2009). Specifically, botallackite, clinoatacamite, and herbertsmithite exhibit triangular, tetrahedral, and kagome Heisenberg (antiferro)magnetic lattices, respectively, for the $\boldsymbol{S}$ = ½(Cu^{2+}) quantum spin that leads to interesting frustrated magnetism or spin liquid behavior.

Of all the $Cu_2Cl(OH)_3$ polymorphs, atacamite is the most common in nature and

63 botallackite the rarest. From synthesis experiments, Pollard et al. (1989) concluded that
64 clinoatacamite is the most stable phase at room temperature and botallackite the least.
65 Moreover, a number of investigations (e.g., Jambor et al. 1996; Braithwaite et al. 2004;
66 Yoder et al. 2011) have demonstrated that, while atacamite and botallackite are very
67 resistant to Zn substitution, clinoatacamite can incorporate up to 6% Zn apfu into its
68 structure if large Zn concentrations are available during formation. The Zn-stabilized
69 paratacamite and herbertsmithite can accommodate up to Zn/Cu = 14% and 33%,
70 respectively. This paper presents a single-crystal X-ray diffraction and Raman
71 spectroscopic study on a botallackite-type compound with Zn/Cu = 100%,
72 $CuZnCl(OH)_3$, the highest Zn content ever reported for the atacamite group of minerals.
73

74 **EXPERIMENTAL METHODS**

75 The $CuZnCl(OH)_3$ sample used in this study was found on a coiled copper wire of
76 unknown age from the Rowley mine, Maricopa County, Arizona, USA and has been
77 deposited in the RRUFF Project with the deposition number R140401
78 (http://rruff.info/R140401). The $CuZnCl(OH)_3$ crystals are blue and platy, up to 0.12 ×
79 0.10 × 0.03 mm (Fig. 1). Associated minerals include simonkolleite $Zn_5(OH)_8Cl_2·H_2O$,
80 wulfenite $PbMoO_4$, hemimorphite $Zn_4Si_2O_7(OH)_2·H_2O$, barite $BaSO_4$, quartz, fluorite,
81 and fibrous crystals tentatively identified by SEM-EDS as $Zn_9(SO_4)_2(OH)_{12}Cl_2·6H_2O$.
82 Barite, quartz, and fluorite occur as single crystals typically > 0.1 mm in size, unevenly
83 distributed over the wire. They, along with copper from the wire, are overgrown by fine
84 iron oxides with substantial Zn concentrations and by crystals of the Cu-Zn salts. Since
85 barite, quartz, and fluorite are all reported from the gangue mineral assemblage in the
86 Rowley mine (Wilson and Miller 1974), the mineralogical and textural evidence suggests
87 that they were dropped onto the wire and cemented in place by authigenic iron oxides and
88 Cu-Zn salts, rather than having precipitated from solution.
89 The chemical composition of the $CuZnCl(OH)_3$ sample was determined with a
90 Cameca SX-100 electron microprobe operated at 20 keV and 18 nA with a beam size of 1
91 µm. The standards include cuprite for Cu, ZnO for Zn, and scapolite for Cl. The average

of 6 analysis points gives (wt.%) CuO = 34.43(29), ZnO = 39.75(19), Cl = 16.09(16), with the total = 90.27(33). The chemical formula was calculated on the basis of 4 (O + Cl) atoms per formula unit, as determined from the structure refinement (Table 2), by adding 12.51 wt.% H_2O to bring the total close to the ideal value, yielding $Cu_{0.94}Zn_{1.06}Cl_{0.99}(OH)_{3.01}$, which can be simplified as $CuZnCl(OH)_3$.

Single-crystal X-ray diffraction data of the $CuZnCl(OH)_3$ sample were collected from a crystal with size $0.05 \times 0.04 \times 0.03$ mm on a Bruker X8 APEX2 CCD X-ray diffractometer equipped with graphite-monochromatized MoKα radiation. Reflections with $I > 2\sigma(I)$ were indexed based on a monoclinic unit cell (Table 1). No satellite or super-lattice reflections were observed. The intensity data were corrected for X-ray absorption using the Bruker program SADABS. The systematic absences of reflections suggest possible space group $P2_1$ or $P2_1/m$. The crystal structure was solved and refined using SHELX97 (Sheldrick 2008) based on the space group $P2_1/m$, because it yielded better refinement statistics in terms of bond lengths and angles, atomic displacement parameters, and *R* factors. The positions of all atoms were refined with anisotropic displacement parameters, except for H atoms, which were refined with the isotropic displacement parameter only. During the structure refinements, ideal chemistry was assumed. Because of similar X-ray scattering powers between Cu and Zn, a direct refinement of their ratios at each individual site was unsuccessful. Therefore, we tested three different models with fixed site occupancies for Cu and Zn at the two distinct octahedral sites, M1 and M2. Model 1 assumed Zn to occupy the M1 site only and Cu M2, which resulted in $R_1 = 0.0183$, and bond-valence sums of 1.95 and 2.05 v.u. for Zn and Cu, respectively. In model 2, Zn was assigned to M2 and Cu to M1, yielding $R_1 = 0.0191$, and bond-valence sums of 2.18 and 1.83 v.u. for Zn and Cu, respectively. Model 3 assumed a random occupation of Zn and Cu [i.e., (0.5Zn + 0.5Cu)] at each site, which produced results between those from models 1 and 2. Consequently, model 1 was adopted in this study. Final refined atomic coordinates and displacement parameters are listed in Table 2 and selected bond lengths and angles in Table 3.

The Raman spectrum of the $CuZnCl(OH)_3$ crystal was collected from a randomly oriented crystal on a Thermo Almega microRaman system, using a 532-nm solid-state laser with a thermoelectric cooled CCD detector. The laser is partially polarized with 4 cm^{-1} resolution and a spot size of 1 μm.

RESULTS AND DISCUSSION

Crystal Structure

The $CuZnCl(OH)_3$ compound is isostructural with botallackite (Hawthorne 1985). Its structure is characterized by brucite-type octahedral sheets made of two distinct octahedra, M1 and M2 (Fig. 2). The M1 octahedron is occupied by Zn^{2+} and coordinated by (5OH + 1Cl), whereas M2 is filled with Cu and coordinated by (4OH + 2Cl). Both octahedra are considerably distorted, with four short equatorial bonds in a square-planar arrangement and elongated axial bonds involving Cl and one OH. The octahedral sheets are parallel to (100) and connected by hydrogen bonding between O atoms of one sheet and the Cl atoms of the adjacent sheet (O—H···Cl) (Fig. 3). Each Cl atom is involved in three hydrogen bonds (or so-called trimeric H-bonds).

The principal structural difference between $CuZnCl(OH)_3$ and botallackite consists in the complete substitution of non-Jahn-Teller distorting Zn^{2+} for Cu^{2+} in the M1 site. As a consequence, the M1 octahedron in $CuZnCl(OH)_3$ is noticeably less distorted than that in botallackite, as measured by the octahedral angle variance (OAV) and quadratic elongation (OQE) (Robinson et al. 1971) (Table 3). The OAV and OQE indices for M1 in $CuZnCl(OH)_3$ are 121.8 and 1.048, respectively, but 135.5 and 1.076 in botallackite. Despite this difference, the M1 octahedron in $CuZnCl(OH)_3$ is still markedly distorted in terms of OAV, indicating that this site is actually angle-distorted, rather than Jahn-Teller-distorted, in contrast to the suggestion by Braithwaite et al. (2004). Similar angle-distorted sites also exist in atacamite, clinoatacamite, paratacamite, and herbertsmithite. According to Braithwaite et al. (2004), Cu^{2+} in such angle-distorted sites is rather susceptible to substitution by non-Jahn-Teller distorting divalent cations of similar radii, such as Zn^{2+}, Ni^{2+}, Co^{2+}, Fe^{2+}, Cd^{2+}, and Mg^{2+}, which is evidently

substantiated by our results.

It is interesting to note the significant discrepancies in all unit-cell parameters between $CuZnCl(OH)_3$ and botallackite (Table 1). Specifically, the unit-cell parameters *a*, *c*, and β for $CuZnCl(OH)_3$ are smaller, whereas the *b* dimension is greater than the corresponding ones for botallackite. These results differ from those for the synthetic Br-analogue of Zn-bearing botallackite, $(Cu,Zn)_2Br(OH)_3$, which allows the Zn substitution for Cu up to the Zn/Cu ratio = 33% (Yoder et al. 2011). With increasing Zn content in the $(Cu,Zn)_2Br(OH)_3$ solid solution, the unit-cell parameters *a* and *b* decrease linearly, but *c* increases linearly and the β angle is essentially unchanged.

Raman spectroscopy

There have been several Raman spectroscopic studies on botallackite, as well as other $Cu_2Cl(OH)_3$ polymorphs, and detailed assignments of major Raman bands have been proposed (e.g., Frost et al. 2002; Martens et al 2003; Liu et al. 2011a, 2011b, 2012). Figure 4 shows the Raman spectrum of $CuZnCl(OH)_3$, along with that of botallackite from the RRUFF Project (R070066) for comparison. The strong bands between 3450 and 3600 cm^{-1} are due to the O-H stretching vibrations and those between 650-1000 cm^{-1} to the Cu-O-H bending vibrations (Liu et al. 2011a, 2011b). The bands ranging from 400 to 520 cm^{-1} can be ascribed to the Cu-O stretching modes and those from 300 to 400 cm^{-1} to the O-Cu-O bending modes. The bands below 250 cm^{-1} are associated with the Cu-Cl interactions and the lattice vibrational modes.

Compared to botallackite, the two strong peaks related to the O-H stretching vibrations for $CuZnCl(OH)_3$ are shifted to higher wavenumbers with a much smaller separation between their peak positions. This observation indicates that the hydrogen bonds in $CuZnCl(OH)_3$ are longer (and thus weaker) and more similar to each other than the corresponding ones in botallackite, in accordance with the structural data from the X-ray diffraction analyses (Table 3).

Geochemical factors in Cu-Zn-Cl salt formation

The overgrowth of the corroded wire and the "detrital" quartz, fluorite, and barite by Cu-Zn-Cl(-S) salts and iron oxides suggests that the wire lay submerged in saline water with locally high concentrations of Cu, Fe, Zn, and S. There are abundant pyrite, chalcopyrite, and accessory sphalerite in the Rowley mine, all of which can readily dissolve in oxidizing water (Welty et al., 1985), thus becoming the supply of Cu, Fe, Zn, and S for the mineral assemblage observed on the wire. It is also possible that some of Fe and Zn came from corroded galvanized steel tools or machine parts left by miners. The sulfides and/or the galvanized steel dissolved or corroded in salty water in the mine and re-precipitated onto the wire as $CuZnCl(OH)_3$ and simonkolleite. This mineralogy suggests that the water was too chloride-rich to stabilize malachite $Cu_2CO_3(OH)_2$, smithsonite $ZnCO_3$, and other Cu- or Zn-bearing minerals that are nominally stable under near-surface, oxidized conditions (Garrels, 1954; Mann and Deutscher, 1980), causing the metals to precipitate as atacamite-group minerals. However, this does not explain the extreme Zn enrichment in $CuZnCl(OH)_3$.

Experiments by Jambor et al. (1996) determined that Zn enrichment in botallackite-structured minerals is favored when the Zn is present as aqueous Zn nitrate rather than a Zn chloride. But when the concentration of Zn nitrate was increased to the maximum possible without precipitating Zn-rich gerhardtite [$(Cu,Zn)NO_3OH$], the botallackite produced had only 9% Zn, which is far short of the Zn content in $CuZnCl(OH)_3$ found at the Rowley mine. However, their results suggest that the nature of Zn^{2+} complexation in solution may be a significant factor in stabilizing different compositions with the botallackite structure. Further experimental work on the aqueous geochemistry of Zn with various anion complexes may be necessary to determine and quantify this effect.

It is likely that a natural occurrence of $CuZnCl(OH)_3$ will eventually be discovered. Atacamite-group minerals have been found lining the cell walls of algal spores around hydrothermal vents on the ocean floor, with the implication that algal sorption of Cu^{2+}, combined with a low sulfide activity and high chloride activity, had induced primary precipitation of atacamite (Mossman and Heffernan, 1978). Divalent Zn also sorbs onto

algal matter, so it is possible that Cu- and Zn-rich waters around algae could produce primary $CuZnCl(OH)_3$. However, it may be difficult to detect, since atacamite-group minerals are highly soluble in fresh water and tend to dissolve after formation except in very arid environments (Cameron et al., 2007).

One of the likeliest places to find $CuZnCl(OH)_3$ may be the Antarctic, where Cu, Fe, and Pb salts are known to form at the surface when marine aerosols corrode exposed sulfides and the absence of liquid water preserves the salts from later dissolution. Atacamite, paratacamite, malachite, antlerite, and other highly soluble Cu salts have all been reported from the Ellsworth Mountains (Vennum and Nishi, 1992). The discovery of botallackite-structured $CuZnCl(OH)_3$ in the Rowley mine clearly shows that botallackite-structured minerals can be stable at near-surface conditions, suggesting that $CuZnCl(OH)_3$ could be present at or near the land surface in an environment where there is no rainfall to dissolve it.

IMPLICATIONS

All previous studies have shown that botallackite is the least stable of all basic copper hydroxylchloride polymorphs and, like atacamite, it is the least prone to the substitution of Zn^{2+} for Cu^{2+}, even under forcing conditions — the presence of large to swamping excesses of Zn^{2+} during its formation (e.g., Jambor et al. 1996; Scott 2000; Braithwaite et al. 2004; Yoder et al. 2011). Therefore, the discovery of the new $CuZnCl(OH)_3$ compound, on the one hand, calls for further research on the formation mechanisms of botallackite-type materials. Such investigations will undoubtedly shed light on the nature of corrosion of Cu-bearing materials, bronze, and other copper-bearing alloys. For example, if further research can identify the factors that lead to Zn-enrichment in botallackite-type minerals, it may be possible to constrain the composition and the source of the fluids that caused the corrosion. On the other hand, it suggests that more botallackite-type compounds or minerals with the chemical formula $Cu\mathit{M}Cl(OH)_3$ (M = Ni^{2+}, Co^{2+}, Fe^{2+}, Mn^{2+}, Cd^{2+}, and Mg^{2+}) may be synthesized or found in nature, as those for the herbertsmithite-type compounds with the chemical formula $Cu_3\mathit{M}Cl_2(OH)_6$

[herbertsmithite (M = Zn), gillardite (M = Ni), leverettite (M = Co), and tondiite (M = Mg)]. In fact, the new botallackite-type mineral, iyoite $CuMnCl(OH)_3$, has been recently reported (Nishio-Hamane et al. 2014). The discovery of the new $CuZnCl(OH)_3$ compound also begs the question whether materials with the chemistry $Cu\mathit{M}Cl(OH)_3$ and the more stable atacamite-type structure could exist naturally or be synthesized, as atacamite also possesses a highly angle-distorted octahedral site that is coordinated by (5OH + 1Cl) with the OAV and OQE values of 136.2 and 1.067, respectively (Parise and Hyde 1986), just as the one in botallackite.

The discovery of the new $CuZnCl(OH)_3$ compound also has implications for the composition of supergene waters in hyper-arid environments, particularly the Atacama Desert. The occurrence of atacamite- and paratacamite-group minerals in the supergene zones of Andean porphyries has been used as evidence for the involvement of saline formation waters in supergene alteration, in contrast to the normal meteoric-dominated supergene waters (Arcuri and Brimhall, 2003; Cameron et al., 2007). If the $CuZnCl(OH)_3$ compound or other Zn-enriched minerals are discovered around ore deposits' supergene zones, they may suggest nitrate- and Zn-rich solutions were also involved. Because nitrate-rich and Zn-rich solutions are not very common in groundwater, this will considerably restrict the possible range of compositions, and therefore the possible origins, of the fluids involved in supergene alteration in hyper-arid climates. Similar considerations apply to botallackite-structured compounds of Cu with Ni^{2+}, Mg^{2+}, Co^{2+}, and other divalent cations capable of substituting for divalent Zn in botallackite.

ACKNOWLEDGEMENTS

We thank Robert Jenkins, Keith Wentz, and Joe Ruiz for providing the $CuZnCl(OH)_3$ specimens. The funding supports from the Science Foundation Arizona and Sao Paulo Research Foundation (Grant: 2013/03487-8) are gratefully acknowledged.

REFERENCES CITED

Alejandre, F.J. and Márquez, G. (2006) Copper-zinc hydroxychlorides: origin and occurrence as paint pigments in Arcos de la Frontera's Chapel of Mercy (Spain). European Journal of Mineralogy, 18, 403-409.

Arcuri, T., and Brimhall, G. (2003) The chloride source for atacamite mineralization at the Radomiro Tomic porphyry copper deposit, northern Chile. Economic Geology, 98, 1667-1681.

Braithwaite, R.S.W., Mereiter, K., Paar, W.H. and Clark, A.M. (2004) Herbertsmithite, $Cu_3Zn(OH)_6Cl_2$, a new species, and the definition of paratacamite. Mineralogical Magazine, 68, 527-539.

Cameron, E.M., Leybourne, M.I., and Palacios, C. (2007) Atacamite in the oxide zone of copper deposits in northern Chile: involvement of deep formation waters? Mineralium Deposita, 42, 205-218.

Fleet, M.E. (1975) The crystal structure of paratacamite, $Cu_2(OH)_3Cl$. Acta Crystallographica, B31, 183-187.

Frost, R.L., Martens, W., Kloprogge, J.T., and Williams, P.A. (2002) Raman spectroscopy of the basic copper chloride minerals atacamite and paratacamite: implications for the study of copper, brass and bronze objects of archeological significance, Journal of Raman Spectroscopy, 33, 801-806.

Garrels, R.M. (1954) Mineral species as functions of pH and oxidation-reduction potentials, with special reference to the zone of oxidation and secondary enrichment of sulphide ore deposits. Geochimica et Cosmochimica Acta 4, 153-168.

Grice, J.D., Szymanski, J.T. and Jambor, J.L. (1996) The crystal structure of clinoatacamite, a new polymorph of $Cu_2(OH)_3Cl$. The Canadian Mineralogist, 34, 73-78.

Hawthorne, F.C. (1985) Refinement of the crystal structure of botallackite. Mineralogical Magazine, 49, 87-89.

Jambor, J.L., Dutrizac, J.E., Roberts, A.C., Grice, J.D. and Szymanski, J.T. (1996) Clinoatacamite, a new polymorph of $Cu_2(OH)_3Cl$, and its relationship to paratacamite and ‘‘anarakite’’. Canadian Mineralogist, 34, 61-72.

Krause, W., Bernhardt, H.J., Braithwaite, R.S.W., Kolitsch, U., Pritchard, R. (2006) Kapellasite, $Cu_3Zn(OH)_6Cl_2$, a new mineral from Lavrion, Greece, and its crystal structure. Mineralogical Magazine, 70, 329-340.

Lichtenegger, H.C., Schöberl, T., Bartl, M.H., Waite, H., and Stucky, G.D. (2002) High abrasion resistance with sparse mineralization: Copper biomineral in worm jaws. Science, 298, 389-392.

Liu, X., Hagihala, M., Zheng, X., Guo, Q. (2011a) Vibrational spectroscopic properties of botallackite-structure basic copper halides. Vibrational Spectroscopy, 56, 177-183.

Liu, X., Meng, D., Hagihala, M., and Zheng, X. (2011b) Microstructural hydroxyl environments and Raman spectroscopy in selected basic transition-metal halides. Chinese Physics, B20, 087801 (1-8).

Mann, A.W. and Deutscher, R.L. (1980) Solution geochemistry of lead and zinc in water containing carbonate, sulphate and chloride ions. Chemical Geology, 29, 293-311.

Martens, W., Frost, R.L., and Williams, P.A. (2003) Raman and infrared spectroscopic study of the basic copper chloride minerals - implications for the study of the copper and brass corrosion and "bronze disease", Neues Jahrbuch für Mineralogie, Abhandlungen, 178, 197-215.

Mossman, D.J., and Heffernan, K.J. (1978) On the possible primary precipitation of atacamite and other metal chlorides in certain stratabound deposits. Chemical Geology, 21, 151-159.

Nishio-Hamane, D., Momma, K., Ohnishi, M., Shimobayashi, N., Miyawaki, R., Tomita, N., and Minakawa, T. (2014) Iyoite, IMA 2013-130. CNMNC Newsletter No. 20, June 2014, page 552; Mineralogical Magazine, 78, 549-558

Parise, J.B. and Hyde, B.G. (1986) The structure of atacamite and its relationship to spinel. Acta Crystallographica, C42, 1277-1280.

Pollard, A.M., Thomas, R.G., and Williams, P.A. (1989) Synthesis and stabilities of the basic copper (II) chlorides atacamite, paratacamite, and botallackite. Mineralogical Magazine, 53, 557-563.

Robinson, K., Gibbs, G.V., and Ribbe, P.H. (1971): Quadratic elongation, a quantitative measure of distortion in coordination polyhedra. Science, 172, 567–570.

Scott, D.A. (2000) A review of copper chlorides and related salts in bronze corrosion and as painting pigments. Studies in Conservation, 45, 39-53.

Sheldrick, G. M. (2008). A short history of SHELX. Acta Crystallographica, A64, 112-122.

Takeda, S., Maruta, G., Terasawa, K., Fukuda, N., and Yamaguchi, K. (1999) Local magnetic Structure of layered compounds $Cu_2(OD)_3X$ with exchangeable acid anion X studied by solid state high resolution deuterium NMR. Molecular Crystals and Liquid Crystals Science and Technology, 335, 11-21.

Vennum, W.R., and Nishi, J.M. (1992) Chemical weathering of Cu, Fe, and Pb sulfides, southern Ellsworth Mountains, West Antarctica. In Webers, G.F., Craddock, C., and Splettstoesser, J.F., Geology and Paleontology of the Ellsworth Mountains, West Antarctica: Boulder, CO, Geological Society of America Memoir, 170, 433-442.

Welty, J.W., Spencer, J.E., Allen, G.B., Reynbolds, S.J., and Trapp, R.A. (1985) Geology and production of Middle Tertiary mineral districts in Arizona. Arizona Bureau of Geology and Mineral Technology Open-File Report 85-1.

Wilson, W. E., and Miller, D. K. (1974) Minerals of the Rowley mine. Mineralogical Record, 5, 10-30.

Yoder, C.H., Schaeffer, R.W., McCaffrey, P.F., Rowand, A., Liu, X., and Schaeffer, J. (2011) The synthesis of copper/zinc solid solutions of hydroxyl carbonates, sulphates, nitrates, chlorides and bromides. Mineralogical Magazine, 75, 2573-2582.

Zheng, X.G. and Xu, C.N. (2004) Antiferromagnetic transition in botallackite $Cu_2Cl(OH)_3$. Solid State Communications, 131, 509-511.

Zheng, X.G., Mori, T., Nishiyama, K., Higemoto, W., Yamada, H., Nishikubo, K., and Xu, C.N. (2005) Antiferromagnetic transitions in polymorphous minerals of the natural cuprates atacamite and botallackite $Cu_2Cl(OH)_3$, Physical Review B, 71, 174404-8.

Zheng, X.G., Yamashita, T., Hagihala, M., Fujihala, M., and Kawae, T. (2009) Magnetic transitions in botallackite-structure $Cu_2(OH)_3Br$ and $Cu_2(OH)_3I$. Physica B, 404, 680-682.

352
353 **List of Tables**
354
355 Table 1. Comparison of crystallographic data for botallackite and the $CuZnCl(OH)_3$
356 Compound.
357
358 Table 2. Coordinates and displacement parameters of atoms in the $CuZnCl(OH)_3$
359 Compound.
360
361 Table 3. Comparison of selected interatomic distances and angles in the $CuZnCl(OH)_3$
362 Compound and botallackite.
363
364
365 **List of Figure Captions**
366
367 Figure 1. Back-scattered electron image of the $CuZnCl(OH)_3$ crystals.
368
369 Figure 2. A brucite-type sheet made of two distinct and highly distorted octahedra in the
370 $CuZnCl(OH)_3$ compound.
371
372 Figure 3. Crystal structure of the $CuZnCl(OH)_3$ compound, showing the brucite-type
373 octahedral sheets stacked along [100] and linked together by O—H…Cl
374 hydrogen bonds.
375
376 Figure 4. Raman spectrum of the $CuZnCl(OH)_3$ compound, along with that of
377 botallackite for comparison.
378
379
380
381
382

This is a preprint, the final version is subject to change, of the American Mineralogist (MSA)
Cite as Authors (Year) Title. American Mineralogist, in press.
(DOI will not work until issue is live.) DOI: http://dx.doi.org/10.2138/am-2016-5560

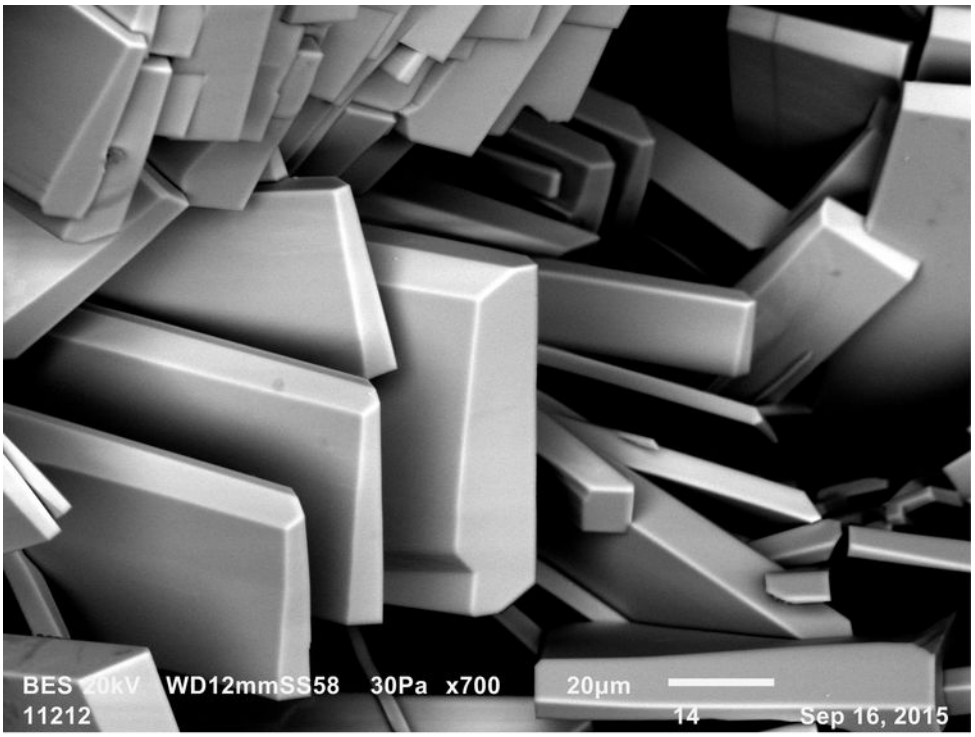

Figure 1

This is a preprint, the final version is subject to change, of the American Mineralogist (MSA)
Cite as Authors (Year) Title. American Mineralogist, in press.
(DOI will not work until issue is live.) DOI: http://dx.doi.org/10.2138/am-2016-5560

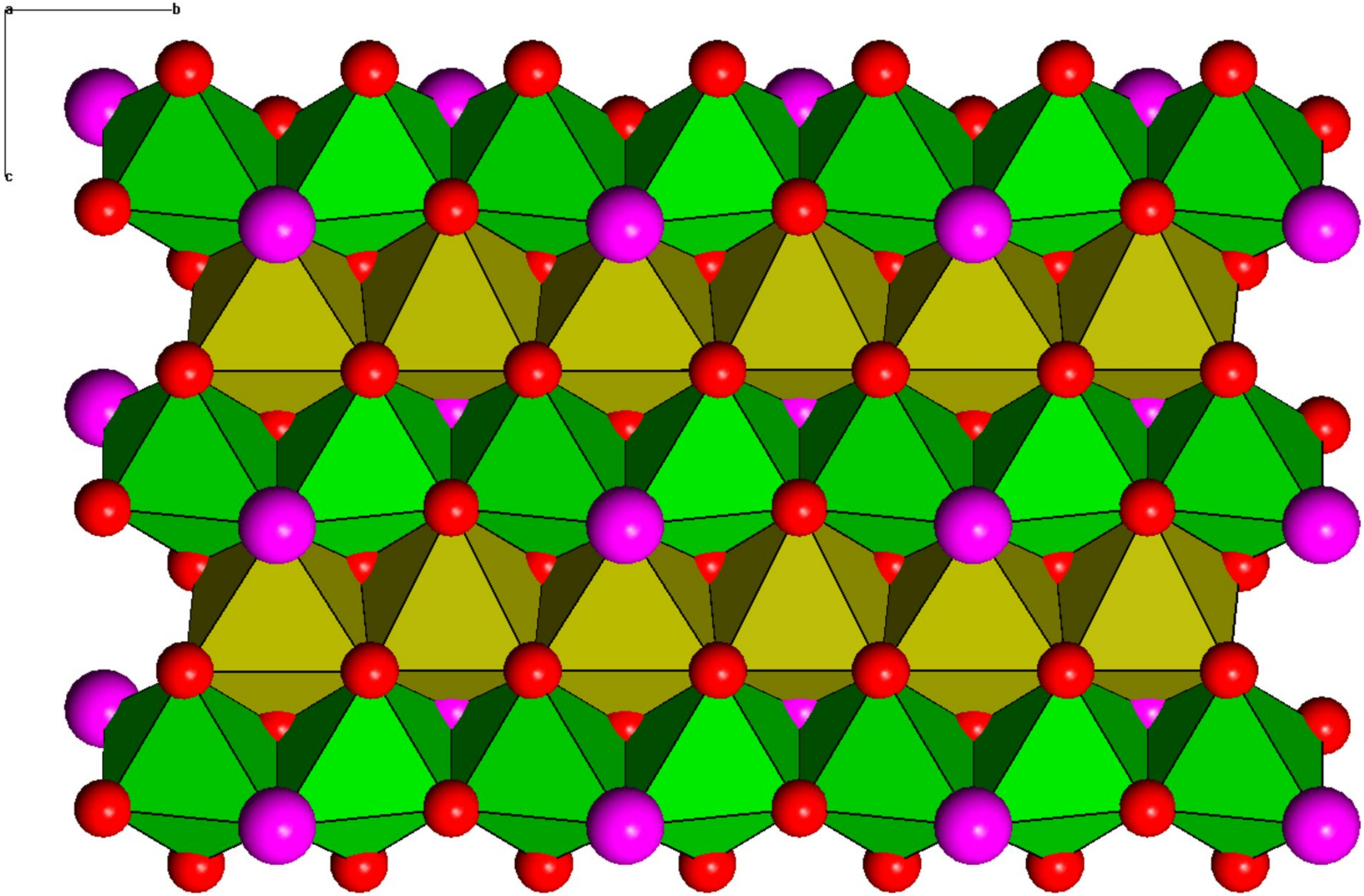

Figure 2

This is a preprint, the final version is subject to change, of the American Mineralogist (MSA)
Cite as Authors (Year) Title. American Mineralogist, in press.
(DOI will not work until issue is live.) DOI: http://dx.doi.org/10.2138/am-2016-5560

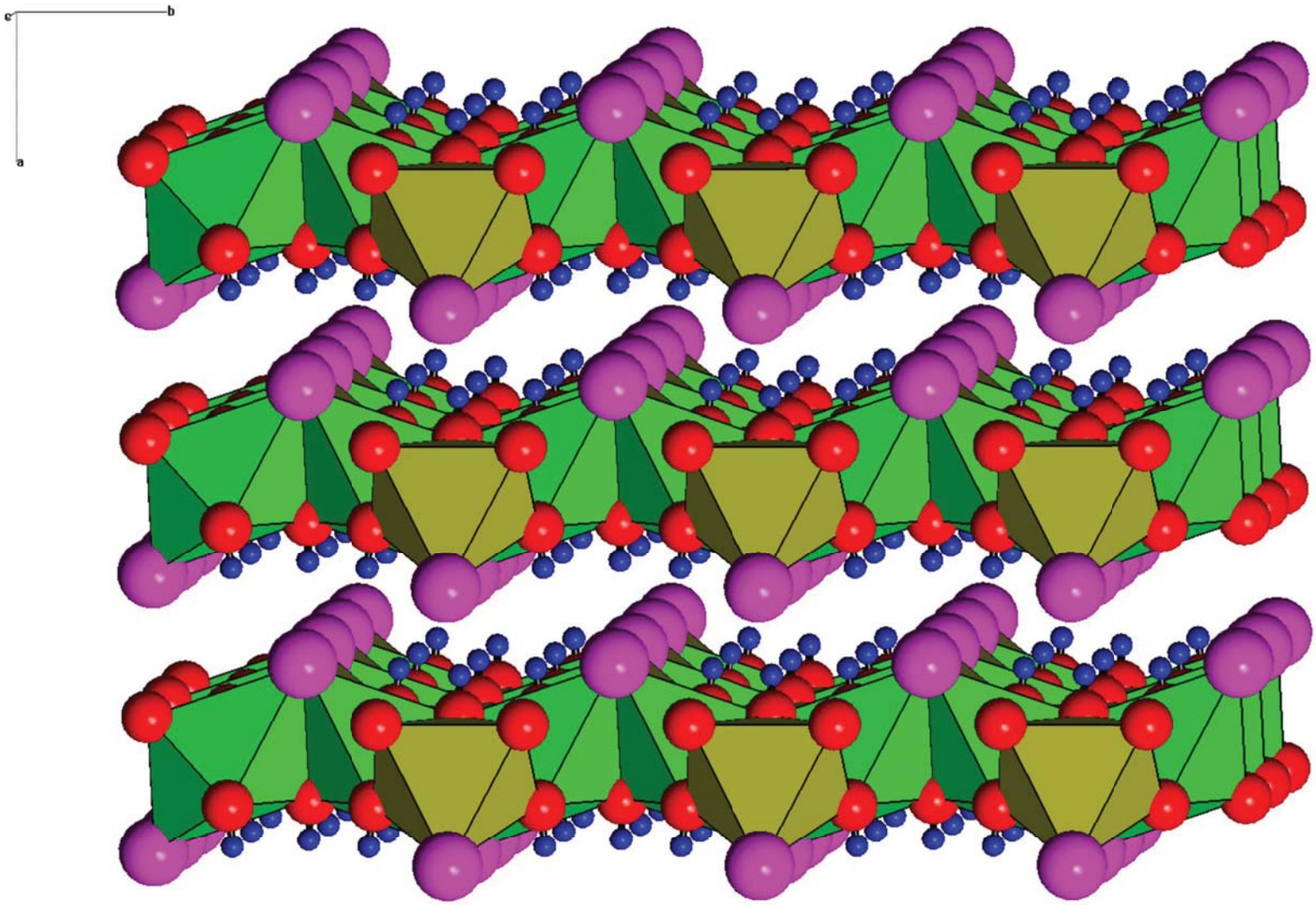

Figure 3

This is a preprint, the final version is subject to change, of the American Mineralogist (MSA)
Cite as Authors (Year) Title. American Mineralogist, in press.
(DOI will not work until issue is live.) DOI: http://dx.doi.org/10.2138/am-2016-5560

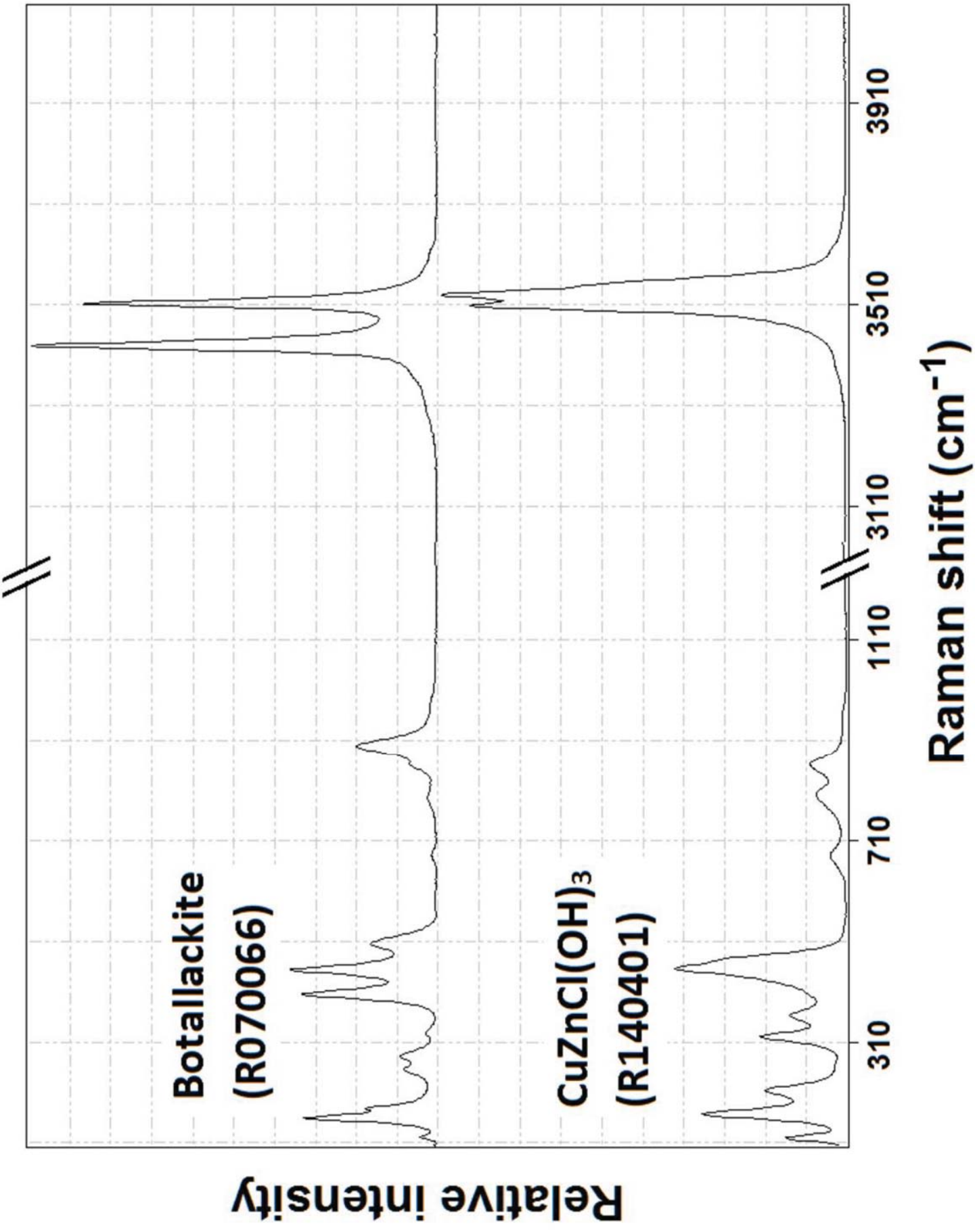

Figure 4

This is a preprint, the final version is subject to change, of the American Mineralogist (MSA)
Cite as Authors (Year) Title. American Mineralogist, in press.
(DOI will not work until issue is live.) DOI: http://dx.doi.org/10.2138/am-2016-5560

Table 1. Comparison of crystallographic data for the new compound $CuZnCl(OH)_3$ and botallackite

	$CuZnCl(OH)_3$	Botallackite
Ideal chemical formula	$CuZnCl(OH)_3$	$Cu_2Cl(OH)_3$
Space group	$P2_1/m$	$P2_1/m$
a (Å)	5.6883(5)	5.717(1)
b (Å)	6.3908(6)	6.126(1)
c (Å)	5.5248(5)	5.636(1)
β (°)	90.832(2)	93.07(1)
V(Å^3)	200.82(3)	197.06(5)
Z	2	2
ρ_{cal}(g/cm^3)	3.56	3.60
λ (Å)	0.71073	0.71073
μ (mm^{-1})	11.769	
2θ range for data collection	≤66.36	≤60
No. of reflections collected	3073	762
No. of independent reflections	813	379
No. of reflections with $I > 2\sigma(I)$	685	358
No. of parameters refined	45	
R(int)	0.021	
Final R_1, wR_2 factors [$I > 2\sigma(I)$]	0.018, 0.033	0.038, 0.042
Final R_1, wR_2 factors (all data)	0.026, 0.035	
Goodness-of-fit	1.042	
Reference	This work	Hawthorne (1985)

Table 2. Coordinates and displacement parameters of atoms in the new compound $CuZnCl(OH)_3$

Atom	*x*	*y*	*z*	U_{eq}	U_{11}	U_{22}	U_{33}	U_{23}	U_{13}	U_{12}
Zn	0.48330(4)	0.25	0.01469(4)	0.0144(1)	0.0245(2)	0.0085(1)	0.0102(1)	0	0.0010(1)	0
Cu	0.5	0	0.5	0.0129(1)	0.0215(2)	0.0093(1)	0.0079(1)	0.0014(1)	-0.0014(1)	-0.0020(1)
Cl	0.1521(1)	0.25	-0.3050(1)	0.0207(2)	0.0170(3)	0.0214(3)	0.0237(3)	0	-0.0020(2)	0
O1	0.6546(3)	0.25	0.3634(3)	0.0148(4)	0.0179(9)	0.0121(7)	0.0143(7)	0	0.0004(6)	0
O2	0.6545(2)	0.0157(2)	0.8210(2)	0.0146(3)	0.0159(6)	0.0147(6)	0.0133(5)	0.0009(4)	0.0003(4)	-0.0004(4)
H1	0.801(6)	0.25	0.381(6)	0.05(1)						
H2	0.802(4)	0.031(3)	0.812(4)	0.021(6)						

Table 3. Selected interatomic distances (Å), angles (°) and other geometrical data in the new compound $CuZnCl(OH)_3$ and botallackite

$CuZnCl(OH)_3$ (This study)			Botallackite (Hawthorne 1985)		
Zn—O2	2.084(1)	×2	Cu1—O2	1.995(6)	×2
—O2	2.090(1)	×2	—O2	1.998(6)	×2
—O1	2.1463(2)		—O1	2.367(9)	
—Cl	2.5636(6)		—Cl	2.732(3)	
Ave.	2.176			2.180	
OAV	121.8			135.5	
OQE	1.048			1.076	
Cu—O1	1.979(1)	×2	Cu2—O1	1.920(5)	×2
—O2	1.970(1)	×2	—O2	2.001(6)	×2
—Cl	2.7733(5)	×2	—Cl	2.789(2)	×2
Ave.	2.241			2.237	
OAV	19.32			17.06	
OQE	1.062			1.066	
O1—H1	0.83(3)			0.8(1)	
H1...Cl	2.63(3)			2.5(1)	
O1—Cl	3.349(2)			3.318(9)	
∠O1—H1...Cl	145(3)°			116(3)°	
O2—H2	0.85(2)			0.6(1)	
H2...Cl	2.52(2)			2.6(1)	
O2—Cl	3.286(2)			3.214(6)	
∠O1—H1...Cl	150(2)°			132(15)°	

Note: OV—Octahedral volume; OAV—Octahedral angle variance; OQE—Octahedral quadratic elongation (Robinson et al. 1971).